

IMECE2023- 111682

**FINITE ELEMENT ANALYSIS AND FATIGUE LIFE PREDICTION OF A LATERALLY
CONDUCTING GAN-BASED POWER PACKAGE UNDER THERMAL CYCLING**

Pouria Zaghari

Department of Mechanical and
Aerospace Engineering
North Carolina State University
Raleigh, NC

Sourish S. Sinha

Department of Electrical and
Computer Engineering
North Carolina State University
Raleigh, NC

Jong Eun Ryu

Department of Mechanical and
Aerospace Engineering
North Carolina State University
Raleigh, NC

Paul D. Franzon

Department of Electrical and Computer
Engineering
North Carolina State University
Raleigh, NC

Douglas C. Hopkins

Department of Electrical and Computer
Engineering
North Carolina State University
Raleigh, NC

ABSTRACT

Thermal fatigue life analysis of GaN packages is an important consideration that affects the reliability and durability of electronic devices. In this paper, the fatigue life assessment of a GaN laterally conducting power packaging, including SAC305 and Sn63/Pb37 solders was conducted using the finite element analysis (FEA) method. The thermal cycling loading was chosen based on JEDEC Standard JESD22-A104D condition M. With temperature cycling from -40°C to 150°C. To simulate the viscoplastic behavior of solder materials under thermal cycling, the Anand constitutive model was adopted. Coffin-Manson, Engelmaier, and Solomon empirical models were utilized to predict the cyclic life of the package based on stress and strain distribution in the solder layers. Results showed that the critical solder joint location of the failure was in the SAC305 solder. The maximum inelastic strain range of SAC305 solder was calculated to be 0.023697. The fatigue life prediction of the module showed that the Engelmaier model was the most conservative model resulting in a fatigue life of 136 cycles.

Keywords: Finite element methods; reliability; fatigue and fracture prediction; stress analysis

1. INTRODUCTION

GaN power semiconductor devices are increasingly being used in various wide-bandgap (WBG) based power modules due to their high power density, high efficiency, and fast switching capabilities compared to traditional silicon (Si)

semiconductors [1]. However, the high-power densities and high operating temperatures of GaN devices can pose several challenges in terms of thermal reliability. Moreover, due to high electron mobility, GaN devices typically have smaller feature sizes than Si devices for the same voltage rating and on-resistance, adversely affecting heat dissipation [2].

Thermal reliability is a critical aspect of power packaging as it directly impacts the performance and lifespan of electronic devices. Excessive increases in the temperature of the power modules could result in reduced power output or even failure. Temperature fatigue, affected by the coefficient of thermal expansion (CTE) mismatch between different materials in the package, is the primary failure mechanism of electronic packages [3], [4]. Therefore, thermomechanical modeling of solder interconnections is an asset to the reliability assessment of the power modules [5].

Different empirical models have been proposed for fatigue life prediction of power devices. These models are based on mechanical stress, strain, and creep parameters of solder joints. Among them, Coffin-Manson [6], [7], Engelmaier [8], and Solomon [9] models are widely used to evaluate the reliability of solder joints under thermal cycling loading. Moreover, various constitutive equations have been proposed, from viscoplastic models to pure time-dependent creep models to simulate the solder behavior. According to the literature, a wide range of solder thermal fatigue life assessments of electronic devices under temperature cycling loading have been conducted. Yan et al. [10] studied the thermal fatigue life of Fan-in Package in

Package by FEA. Wenchao et al. [11] investigated SAC305 solder performance in a multichip packaging module. Wang et al. [12] proposed a study on a ball grid array (PBGA) packaging structure.

This paper aims to analyze the mechanical behavior and predict the fatigue life of a proposed half-bridge module with two laterally conducting GaN power packaging. Mechanical modeling of the SAC305 and Sn63/Pb37 solders in this package was applied using Anand viscoplastic constitutive model [13]. Parameters such as inelastic strain, shear strain, and von Mises stress were investigated for the solder joints by the FEA model. Finally, the output of the FEA model was used to predict the fatigue life and the location of the failure in the power module.

2. METHODOLOGY

2.1. GAN WBG power module structure

In this study, the intelligent power module (IPM) integrates GaN power devices, gate drivers, power, and gate decoupling capacitors. In Fig. 1(a) and Fig. 1(b), the top side of the left GaN die was bonded onto a highly thermally conductive epoxy-resin insulated metal substrate (eIMS) using SAC305. The eIMS was a stack of 4-oz Cu/120 μ m dielectric/2mm baseplate Cu. An ultra-thin organic-based epoxy resin composite dielectric (ERCD) was used as the insulating layer. The back side (substrate) was soldered to a copper (Cu) spacer using Sn63/Pb37. The bonding process was the same for the GaN device on the right side. The Cu spacers acted as the electrical connection of the source to the dies as well as increasing the thermal dissipation of the package. Finally, the module was encapsulated by an epoxy-based encapsulant. Symmetry in heat dissipation and stress management due to CTE mismatch was achieved using the flip-chip arrangement of both dies.

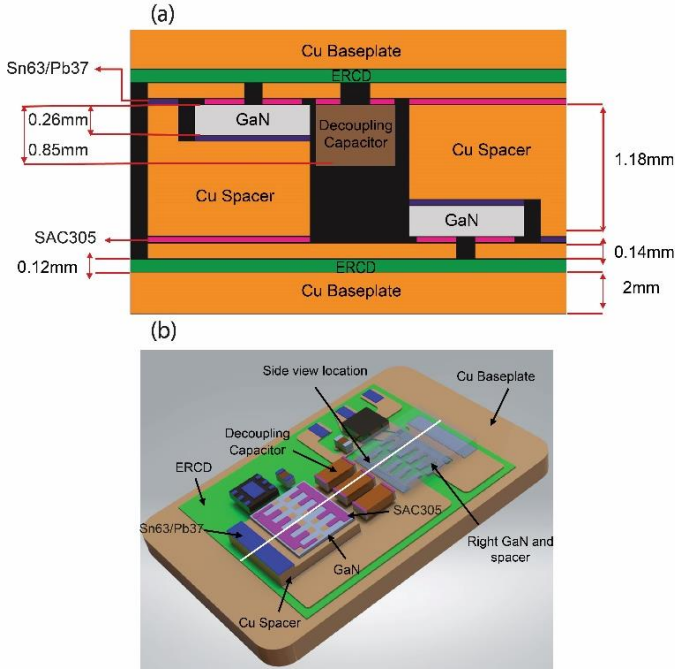


FIGURE 1: (a) 2D SIDE VIEW (b) 3D ISOMETRIC VIEW OF THE GAN IPM

2.2. Material characterization

In this study, all the materials except the solder were considered to behave as isotropic elastic. The required mechanical and thermomechanical properties of these materials are noted in Table 1. Moreover, solder materials were modeled using Anand viscoplastic constitutive model. This model considers inelastic strain and time-dependent creep behavior of materials during the deformation. The flow equation of the Anand model correlating the inelastic strain rate $\dot{\epsilon}_p$ is as follows [5]:

$$\dot{\epsilon}_p = A \exp\left(-\frac{Q}{RT}\right) \left[\sinh\left(\xi \frac{\sigma}{s}\right) \right]^{\frac{1}{m}} \quad (1)$$

In which A is the pre-exponential factor, Q is the activation energy, m is the strain rate sensitivity, T is the temperature, ξ is the stress multiplier, R is the universal gas constant, s is the deformation resistance, and σ is the equivalent von Mises stress. The evolution equation for the internal variable s is as follows:

$$\dot{s} = h(\sigma, s, T) \dot{\epsilon}_p \quad (2)$$

$$h = h_0 \left[1 - \frac{s}{s^*} \right]^a \cdot \text{sgn}\left(1 - \frac{s}{s^*}\right) \quad (3)$$

$$s^* = \hat{s} \left[\frac{\dot{\epsilon}_p}{A} \exp\left(\frac{Q}{RT}\right) \right]^n \quad (4)$$

where \dot{s} is the time derivative of deformation resistance, h is associated with dynamic hardening and recovery, and its initial value is h_0 which is the deformation hardening-softening constant, a is the strain rate sensitivity exponent of hardening, s^* is saturation coefficient, \hat{s} and n are material constants. The constants required for Anand viscoplastic model of the solder materials are listed in Table 2.

TABLE 1: IPM MATERIAL PROPERTIES [10]

Component	Material	Properties		
		Elastic Modulus (GPa)	Poisson's Ratio	CTE (ppm/°C)
Spacer				
Baseplate	Copper	120	0.35	17
Conductor Layer				
Encapsulant	Epoxy	20	0.3	20
Die	GaN	160	0.26	3
Dielectric	ERCD	53	0.22	15
Solder I	SAC305	38.7-0.176T	0.35	21
Solder II	Sn63/Pb37	43.88-0.074T	0.38	23.5

TABLE 2: ANAND CONSTANTS FOR SAC305 AND SN63/PB37 [3], [5]

Symbol	Solder Alloys	
	SAC305	Sn63/Pb37
s^*	46.41	3.1522
$Q/R \left(\frac{1}{K}\right)$	9320	6526
$A \left(\frac{1}{s}\right)$	10000	6220
ξ	5.09	3.33
m	0.16	0.27
h_0 (MPa)	326680	60599
\hat{s} (MPa)	73.2947	36.86
n	0.006	0.022
a	1.74	1.7811

2.3. FEM analysis and simulation conditions

The simulation was implemented by ANSYS software. After importing the CAD model to the software, the material properties and the Anand constants of the solder materials were assigned to each component. Mesh quality has a significant effect on the reliability of the simulation results. To achieve a good quality mesh, a combination of hexahedron and tetrahedral conformal mesh methods were used. The final meshed consisted of 228524 elements and 470359 nodes. The mesh structure is illustrated in Fig. 2.

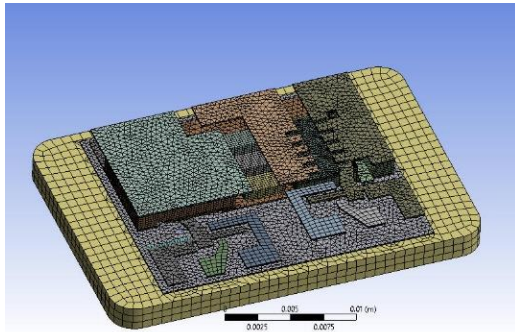


FIGURE 2: IPM GENERATED MESH STRUCTURE (ENCAPSULANT, TOP BASEPLATE AND ERCD ARE HIDDEN)

As shown in Fig.3 The thermal cycling loading was chosen based on JEDEC Standard JESD22-A104D condition M. With temperature cycling from -40°C to 150°C , $15^{\circ}\text{C}/\text{min}$ ramps and 10min dwell time. The get more stable and reliable results, the simulation was done based on six complete cycles.

The mechanical boundary conditions are illustrated in Fig. 4. The boundary conditions were defined as displacement constraints. The IPM was supported such that the y-direction displacements of the top and bottom copper substrates were restricted. Meaning that module was fixed in the y-direction $u(y) = 0$ [3]. To further

restrict the degrees of freedom of the structure a fixed node was considered in the corner of the module.

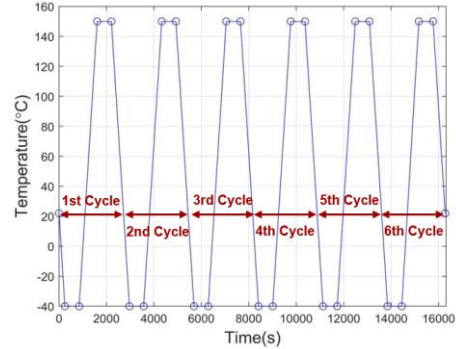


FIGURE 3: TEMPERATURE PROFILE OF THERMAL CYCLIC LOADING

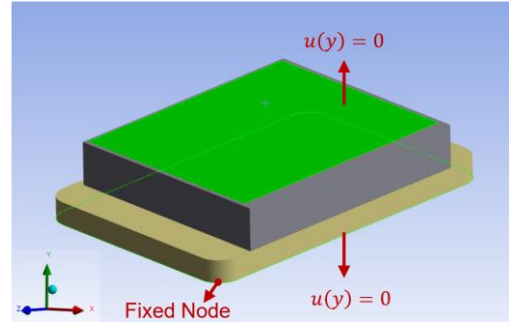


FIGURE 4: BOUNDARY CONDITIONS OF IPM MODULE

2.4. Fatigue life prediction models

Three different strain-based fatigue life prediction models were studied in this research. The Coffin-Manson model is used to estimate the low-cycle fatigue life of solders under temperature cycling. In this model, the fatigue life (N_f) is a function of total inelastic strain of the solder. The Coffin-Manson model is as below [6], [7].

$$N_f = C(\Delta\varepsilon_p)^{-\eta} \quad (5)$$

In which, $\Delta\varepsilon_p$ is the cyclic inelastic equivalent strain range, C and η are empirical constants. For SAC305 solder joints C and η are 0.235, and 1.75 [14]. For Sn63/Pb37 these constants are equal to 0.146 and 1.94 [15].

Engelmaier, modified the Coffin-Manson model by taking the effects of temperature and cycling frequency into account [8].

$$N_f = \frac{1}{2}(\Delta\gamma/2\varepsilon_f)^{1/c} \quad (6)$$

where $2\varepsilon_f$ is the fatigue toughness coefficient, c fatigue exponent, and $\Delta\gamma$ is the cyclic shear strain range, that is $\sqrt{3}\Delta\varepsilon_p$. For SAC305 solder $2\varepsilon_f$ is equal to 0.48 and for lead-based

eutectic solder alloys it is 0.65. The fatigue exponent can also be calculated using the following equation [3], [12].

$$c = -0.442 - 6 \times 10^{-4}T_m + 1.74 \times 10^{-2}\ln(1 + f) \quad (7)$$

T_m is the mean temperature of thermal cycle which is 95°C, and f is the cycle frequency per day that is equal to 31.76cycles/day.

Solomon model considers the effect of plastic shear strain on the fatigue life of solder joint. The expression is as follows [16].

$$N_f^\alpha \Delta\gamma_p = \theta \quad (8)$$

where $\Delta\gamma_p$ is the plastic shear strain range, and α and θ are constants. Based on Solomon's research, α and θ are equal to 0.51 and 1.14 [3].

3. RESULTS AND DISCUSSION

3.1. Stress and strain analysis

The first step in the fatigue prediction of the IPM is to identify the position of the critical solder joint by analyzing the stress and strain. Fig. 5 and Fig. 6 show the inelastic strain and equivalent von Mises stress in the critical location of solders. The critical solder location in SAC305 is the layer between the right spacer and baseplate. The solder layer between the right GaN and the Cu spacer is also the critical location of the Sn63/Pb37 solder. The critical solder locations and the inelastic strain distributions are illustrated in Fig. 7.

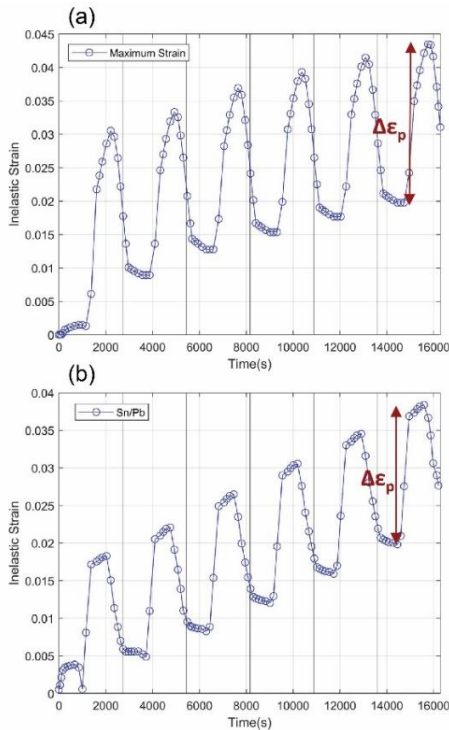


FIGURE 5: MAXIMUM INELASTIC STRAIN IN (a) SAC305 (b) SN63/PB37

From strain analysis in the solder joints, it could be found that the SAC305 critical solder point has a relatively higher inelastic strain in comparison to Sn63/Pb37. The maximum inelastic strain of SAC305 was 0.0435 and in Sn63/Pb37 was calculated to be 0.0384. It can also be seen that the maximum inelastic strain increases by increasing the number of cycles, which could have been predicted by taking the plastic and creep strain effects into the account.

From Fig. 6, it was found that the maximum stress and strain in each cycle happen in the low-temperature phase, however, the minimum stress and strain correspond to high-temperature phase. A decrease in the von Mises stress can also be observed in the dwell times, which corresponds to stress relaxation. The maximum von Mises stress in the solder material (SAC305) was 52.51MPa.

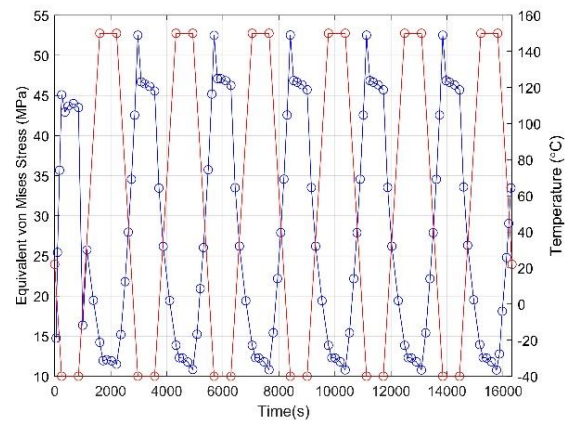


FIGURE 6: MAXIMUM EQUIVALENT VON MISES STRESS IN SOLDER JOINTS (SAC305)

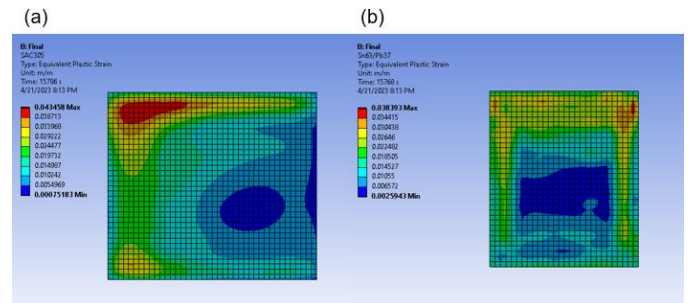


FIGURE 7: MAXIMUM INELASTIC STRAIN LOCATION AND DISTRIBUTION IN (a) SAC305 (b) SN63/PB37

3.2. Fatigue life prediction results

The output of the FEA model was used to perform the fatigue life prediction of the IPM based on the empirical models. Because the constants of the empirical models vary based on the solder material (Except the Solomon model), the life cycle fatigue assessment should be investigated for the critical location of both solders. The fatigue life of the IPM would be the minimum life cycle of the solders. The maximum inelastic strain

range of SAC305 solder was 0.0237 and for the Sn63/Pb37 it was 0.0174. Based on these values, the Thermal fatigue lifetime of the solder joints are presented in Table 3.

It can be seen that for all three models, the fatigue life prediction should be based on SAC305 solder joints. The Engelmaier is the most conservative model. Based on this model, the thermal fatigue life of the IPM is 136 cycles. The discrepancy in the Coffin-Manson and Engelmaier models is attributed to the effects of mean temperature and the thermal cycling frequency which is considered in the Engelmaier equation. We can also conclude that the empirical model constants have a significant effect on the predicted fatigue life cycle. The Solomon empirical model, which was originally used for 60/40 Tin-lead, solder significantly, overestimates the fatigue life of the solders.

TABLE 3: THERMAL FATIGUE LIFETIME OF SOLDERS

Model	N_f (Cycles)	
	SAC305	Sn63/Pb37
Coffin-Manson	164	376
Engelmaier	136	549
Solomon	677	1235

4. CONCLUSION

In this study, FEM analysis of the fatigue life of a GaN wide-bandgap laterally conducting power package module using was investigated. The solder material's mechanical behavior consisting of SAC305 and Sn63/Pb37 was simulated by adopting Anand constitutive viscoplastic model. Based on the results, the thermal fatigue lifetime of solders was estimated to be 136 cycles. Among the fatigue life empirical prediction models, the Engelmaier model was the most conservative model. For future research, studying the effects of solder materials, and thickness of the ERCD and copper spacers to improve and optimize the fatigue lifetime of the power module could be considered as a practical approach.

REFERENCES

- [1] T. J. Flack, B. N. Pushpakaran, and S. B. Bayne, "GaN Technology for Power Electronic Applications: A Review," *Journal of Electronic Materials* 45(6) (2016) 2673–2682.
- [2] D. Kim, C. Chen, S. Nagao, and K. Suganuma, "Mechanical characteristics and fracture behavior of GaN/DBA die-attached during thermal aging: pressureless hybrid Ag sinter joint and Pb–5Sn solder joint," *Journal of Materials Science: Materials in Electronics* 31(1) (2020) 587–598.
- [3] J. A. Depiver, S. Mallik, and E. H. Amalu, "Thermal fatigue life of ball grid array (BGA) solder joints made from different alloy compositions," *Eng Fail Anal.* 125 (2021).
- [4] D. A. Shnawah, M. F. M. Sabri, and I. A. Badruddin, "A review on thermal cycling and drop impact reliability of SAC solder joint in portable electronic products," *Microelectronics Reliability* 52(1) (2012) 90–99.
- [5] M. Calabretta, A. Sitta, S. M. Oliveri, and G. Sequenzia, "Power Semiconductor Devices and Packages: Solder Mechanical Characterization and Lifetime Prediction," *IEEE Access* 9 (2021) 22859–22867.
- [6] L. F. Coffin Jr, "A study of the effects of cyclic thermal stresses on a ductile metal," *Transactions of the American Society of Mechanical Engineers* 76(6) (1954) 931–949.
- [7] S. S. Manson, "Behavior of materials under conditions of thermal stress," (1953).
- [8] W. Engelmaier, "Fatigue Life of Leadless Chip Carrier Solder Joints During Power Cycling," *IEEE Transactions on Components, Hybrids, and Manufacturing Technology* 6(3) (1983).
- [9] H. D. Solomon, "The influence of hold time and fatigue cycle wave shape on the low cycle fatigue of 60/40 solder," in *38th Electronics Components Conference Proceedings*, 1988.
- [10] X. Yan and G. Li, "Study of thermal fatigue lifetime of fan-in package on package (FiPoP) by finite element analysis," in *2009 International Conference on Electronic Packaging Technology & High Density Packaging*, 2009.
- [11] T. Wenchao, Z. Laiqiang, and G. Rongcheng, "Analysis of complex packaging model based on BGA," in *2013 14th International Conference on Electronic Packaging Technology*, 2013.
- [12] W. Wang and X. Long, "Temperature and strain-rate dependent constitutive model for prediction of thermal cycling life," in *IOP Conference Series: Materials Science and Engineering*, Institute of Physics Publishing, 2019.
- [13] L. Zhang, J. G. Han, Y. Guo, and C. W. He, "Anand model and FEM analysis of SnAgCuZn lead-free solder joints in wafer level chip scale packaging devices," *Microelectronics Reliability* 54(1) (2014) 281–286.
- [14] P. H. Chou, H. Y. Hsiao, and K. N. Chiang, "Failure life prediction of wafer level packaging using DoS with AI technology," in *Proceedings - Electronic Components and Technology Conference*, Institute of Electrical and Electronics Engineers Inc., 2019.
- [15] M. Mukai, T. Kawakami, Y. Hiruta, K. Takahashi, K. Kishimoto, and T. Shibuya, "Fatigue Life Estimation of Solder Joints in SMT-PGA Packages," *J Electron Packag.* 120(2) 1998 207–212.
- [16] X. Li, R. Sun, and Y. Wang, "A review of typical thermal fatigue failure models for solder joints of electronic components," in *IOP Conference Series: Materials Science and Engineering*, Institute of Physics Publishing, 2017.